HELMHOLTZ ASSOCIATION
112 | JOINT RESEARCH GROUP

GSI

TECHNISCHE UNIVERSITÄT DARMSTADT

Warm Dense Matter Experiments at GSI

Dieter HH Hoffmann, Eran Nardi[8]

P. Spiller and Lars Bozyk GSI accelerator department
D. Varentsov, A. Hug, S. Udrea, J. Ling
and N.A. Tahir

2010 Ion Beam Driven High Energy Density Workshop
Pleasanton, California, June 22nd – 24th, 2010

S. El Moussati[3], A.Fedenev[4], A.Fertman[2], A.Golubev[2], A. Hug[3], B.Ionita[3], A.Kantsyrev[2], K.Khishchenko[5], A.Khudomyasov[2], M.Kulish[1], J.Ling[3], N.Markov[2], J. Menzel[3], V.Mintsev[1], N. Müller[3], D.Nikolaev[1], A.Pyalling[1], N.Shilkin[1], V.Ternovoi[1], V.Turtikov[2], S.Udrea[3], A.Ulrich[6], D. Varentsov[4], K. Weyrich[4], D.Yuriev[1], Y.Zhao[7]

[1] Institute of Problems of Chemical Physics (IPCP), Chernogolovka, Russia
[2] Institute for Theoretical and Experimental Physics (ITEP), Moscow, Russia
[3] Technische Universität Darmstadt (TUD), Darmstadt, Germany
[4] GSI Helmholtzzentrum für Schwerionenforschung GmbH, Darmstadt, Germany,
[5] Joint Institute for High Temperatures, Moscow, Russia
[6] Physik Department E12, Technische Universität München, Garching, Germany
[7] Institute of Modern Physics, Lanzhou, China
8 Weizmann Institute of Science, Rehovot, Israel


GSI
FAIR

Topics

- Stopping Power of Ions in WDM
- Beam Intensity Issues
- WDM Experiments

Projectile Charge State Dynamics in WDM Experiments

E. Nardi

Stopping power ay proportional to the square on the ion charge.

How does the changing target density effect the ion charge state & hence the stopping.

Case: Li ion on WDM target, beam 1-3 MeV

Two Basic Effects on the Energy Deposition

- **Density effect on the charge state**
  a) " Gas Solid Density Effect" , Bohr Lindhard Model
  Eisenbarth et al. Laser Part. Beams 25, 601 (2007)
  b) Dynamic Screening by Target Plasma Electrons,
  Nardi et al. Laser Part, Beams 27, 355 (2009)

- **Charge State Fluctuations**

Smears energy deposition, effect on shape of Bragg Peak. Zinamon, Nardi & Haas,. NIM B69 127 (1992)

Gas Solid Density Effect:

- Bohr Lindhard Model : Projectile excited states are highly populated for solid target in gas target decay to ground state. Recent calculation by Eisenbarth et al LPB 25, 601 (2007).

- Example for Li ions, experimental: Wittkower & Betz, Atomic Data, 5, 43 (1973)

E(MeV)	Q	Target
2.34	**2.51**	Celluoid
2.34	2.17	He
2.34	2.38	N2
2.34	2.27	Kr
1.18	**1.86**	Celluoid
1.18	1.52	He
1.18	1.73	N2
1.16	1.66	Kr

Gas Solid effect at “intermediate densities” in WDM blow off target

- Gas density 10^{-3} of solid density. In WDM target expansion down to only 10^{-1} of target density

- Effect less pronounced & must be calculated on the basis of the Bohr Lindhard model, Eisenbarth et al. Laser Part. Beams 25, 601 (2007

- Note Lassen “Total charges of fission fragments as functions of pressure of the stopping gas” Dan. Mat. Fys. Medd. 26, 1 (1951)

Effect of dynamic screening by valence electrons on projectile charge state

- Projectile binding energy: reduced by $\Delta E = ze^2/(v/\omega_p)$, z projectile charge, ω_p given by the number of target valence (plasma) electrons.

- Derivation: based on Rogers Graboske & Harwood, PRA 1, 1577 (1970).

- Experimental proof: Chevalier et al. PRA 41, 1738 (1990).

  Velocity threshold for binding of 3p state of He+ on amorphous carbon. Above 1.4 MeV, 3p state bound. Below this, where dynamic screening length is smaller i.e. screening more effective, 3p state does not exist.

Suppression of ionization energy causes increase in charge state by:

- **Increase in ionization cross section,**

  BEA approximation: $\sigma_I = (e^4 Z_t^2 / U_n^2) G(V)$

  U_n, ionization energy of n-th shell, which decreases by ΔE.

- **Decrease in recombination cross section**

  Rc, Bohr Lindhard, “Coulomb recombination radius” becomes smaller.

2 MeV Carbon beam on Carbon target

Nardi et al. Laser & Part. Beams 27, 355 (2009)

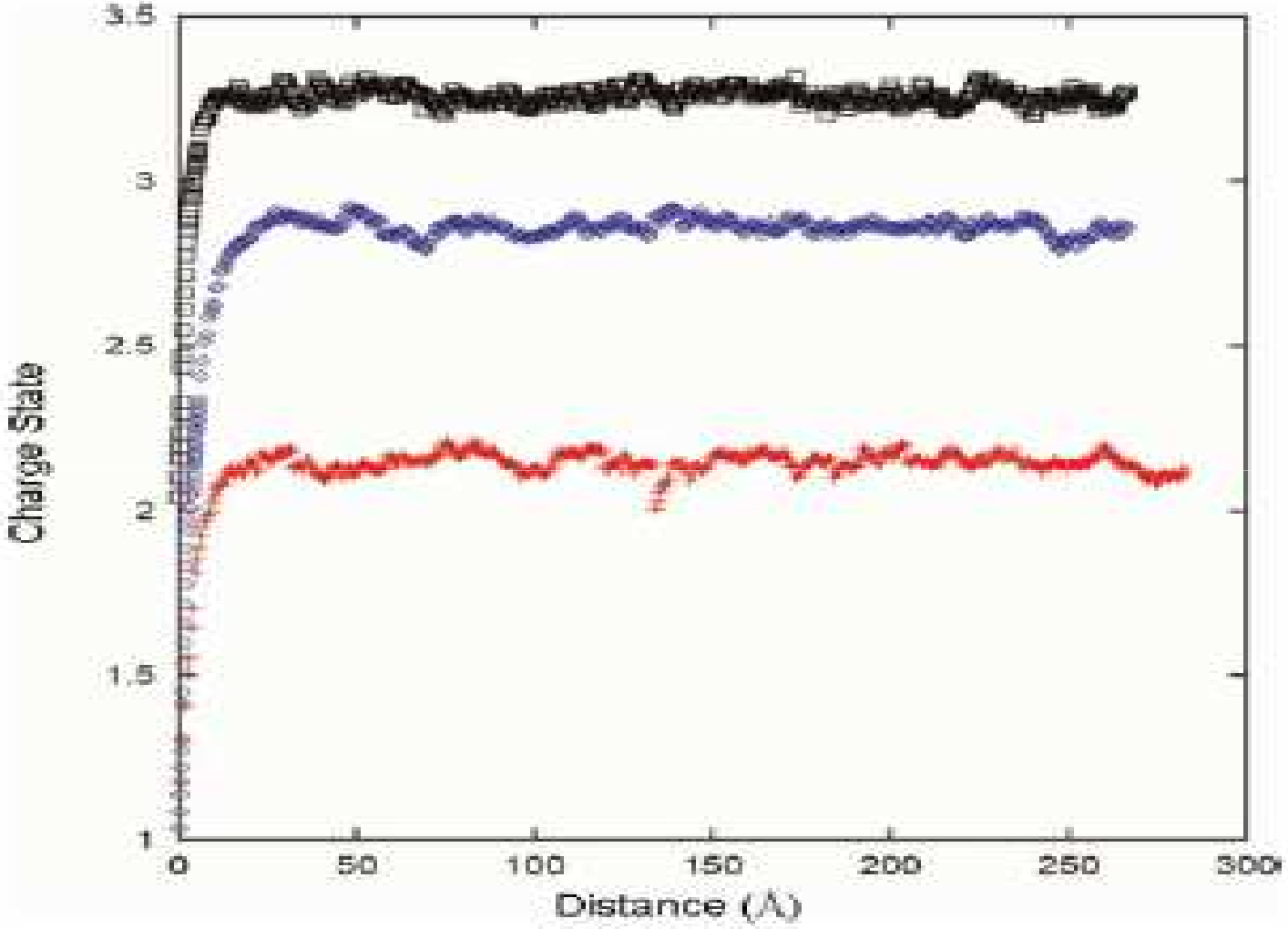

Fig. 1. (Color online) Charge state as a function of penetration depth in a gas target (lower curve), solid target at ambient conditions (middle curve) and for a cold solid target at twice the density of the target at ambient conditions (upper curve). The projectile is carbon at 2 MeV.

Charge State Fluctuations *Smears* Bragg Peak: Iodine ions Z=26+ @ 3MeV/A on Li plasma, T=30eV RO=10^{-3}g/cm^3 from

Zinamon Nardi & Haas, NIMB 69, 127 (1992)

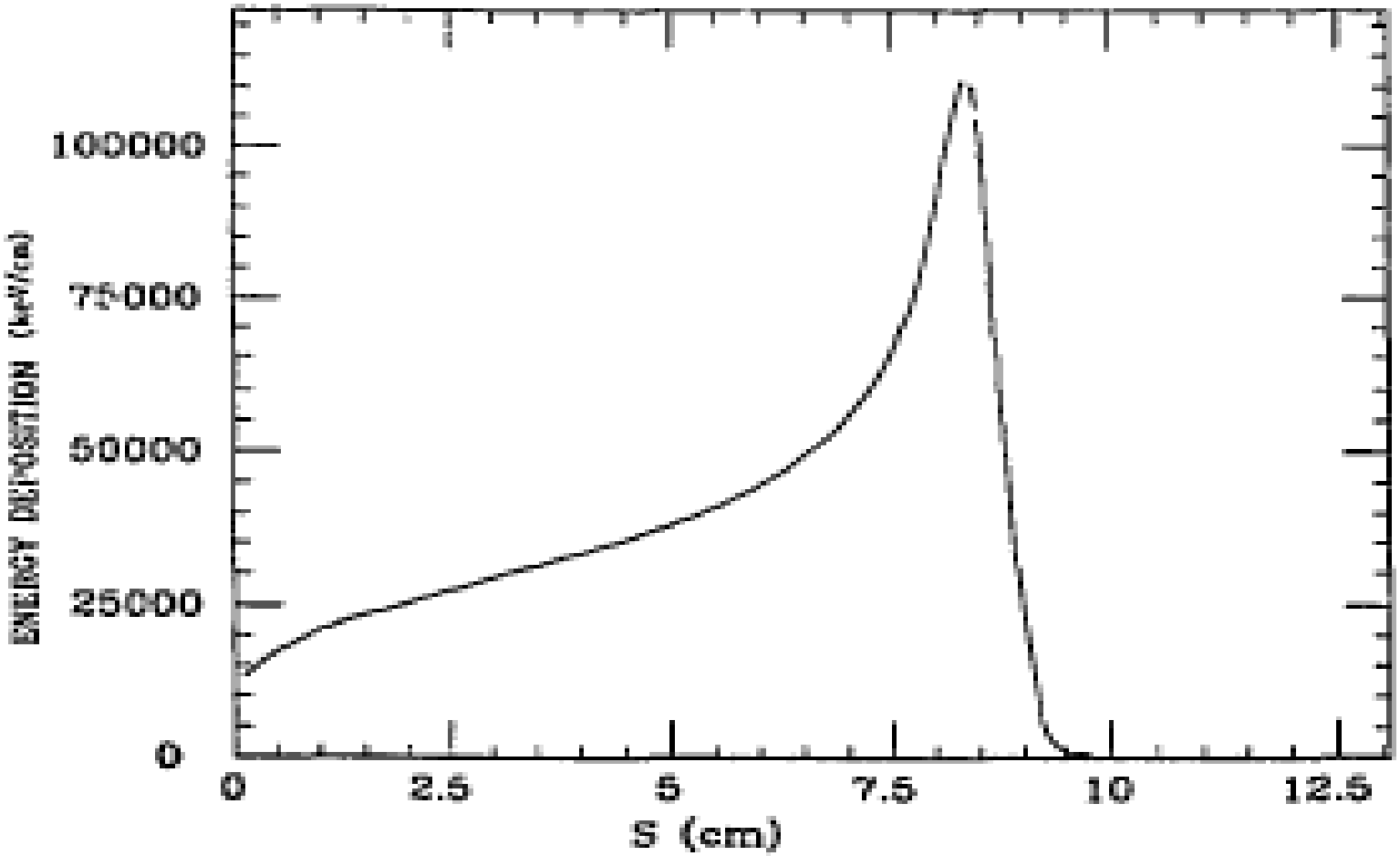

PROGRAM: Calculate charge state dynamics & stopping at the "intermediate" WDM densities

- "Gas Solid Density effect" by Bohr Lindhard model, Eisenbarth et al. Laser Part. Beams 25, 601 (2007)
- "Dynamic Screening effect" on charge state, Nardi, et al., Laser Part, Beams 27, 355 (2009)
- "Charge State Fluctuations" , Zinamon Nardi & Haas, NIMB 69, 127 (1992)

High Intensity Beams for WDM Research at GSI-Synchrotron

- HEDP stands for high intensities
- U^{28+} is used instead of U^{73+} for acceleration to avoid stripping losses
- SIS18 operation with U^{28+} shows fast and intensity dependent beam losses 2001
- Huge pressure rise during operation
- Beam lifetime and pressure depend on each other

Spiller, Bozyk

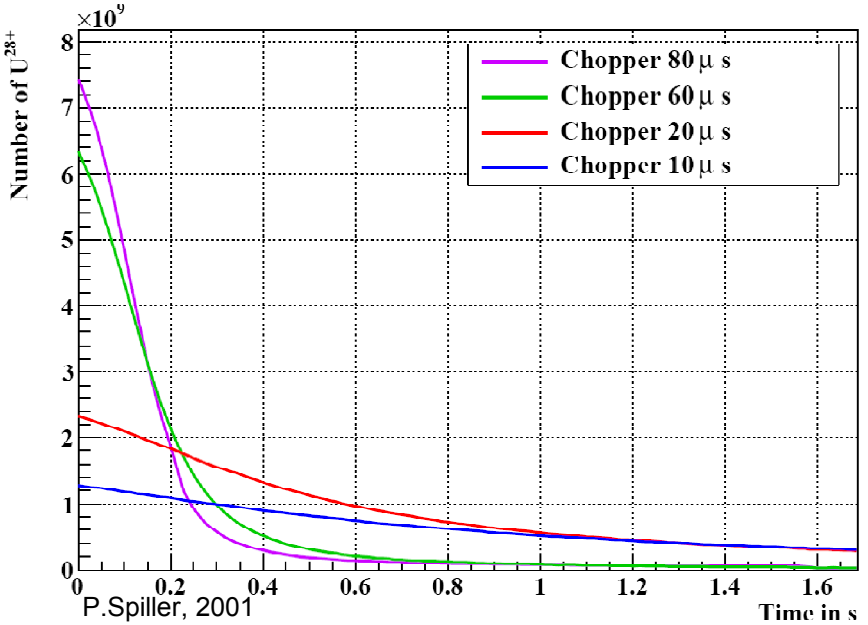

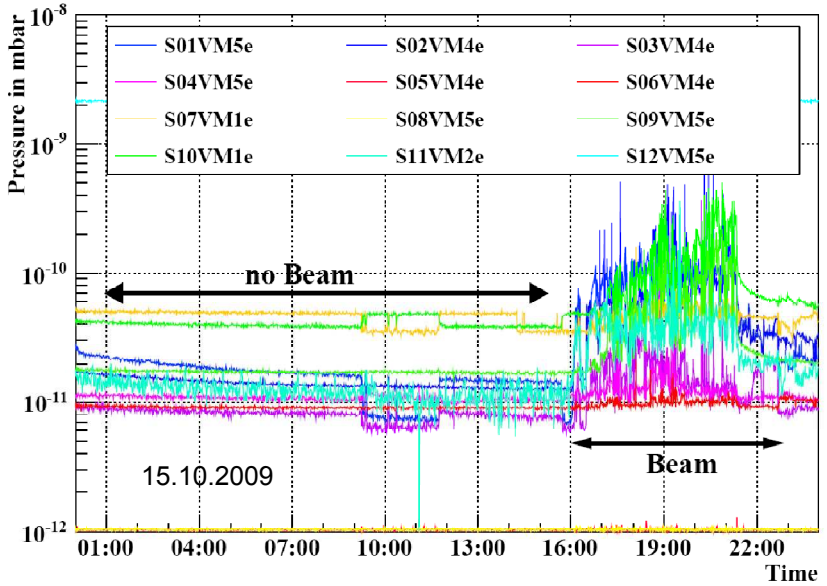

Ionization Loss Mechanisms

All beam losses produce a pressure rise via ion stimulated desorption

- Ionization losses depend on pressure, can also be triggered by other loss mechanisms (see below)
- A vacuum instability may limit the maximum number of particles
- Loss mechanism driving the initial pressure bump:
  - Injection losses
  - HF-Capture
  - Beam dynamic losses: Resonance, space charge, ...
  - Ionization losses in the static vacuum

Charge Exchange Loss Mechanisms

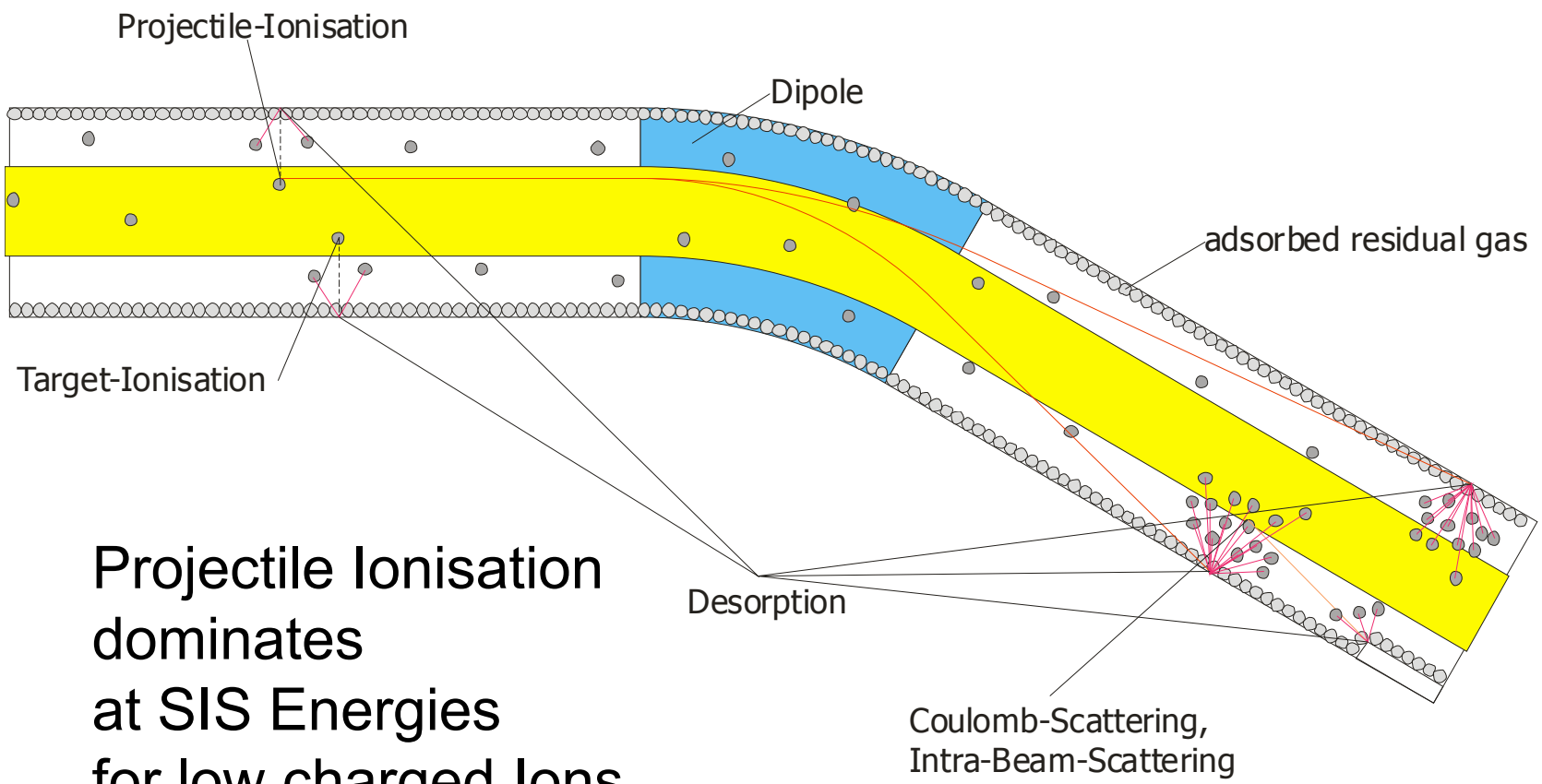

Projectile Ionisation
dominates
at SIS Energies
for low charged Ions

$U^{28+} + R^0 \rightarrow \mathbf{U^{29+}} + R^0 + e^-$

Ion Stimulated Desorption

- On vacuum vessel surfaces residual gas molecules get adsorbed
  - Binding energy few eV
  - Can be released by ion bombardment
- Desorption Rate η
  - Scales with specific energy loss $(dE/dx)^2$ (Max. at SIS18 injection)
  - Depends on angle of incidence
    - $\eta_{\perp} \sim 100$ molecules/Ion
    - $\eta_{\angle} \sim 3...30 \cdot 10^3$ molecules/Ion, not measured at SIS100 energies
  - Perpendicular incidence → Low desorption

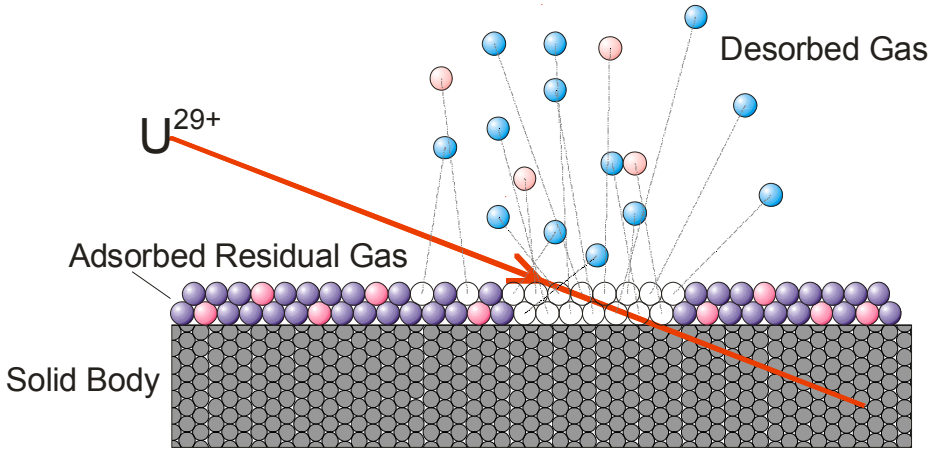

Ionization Cross Sections

- Cross section for charge exchange depends on energy, ion species, charge state and residual gas composition

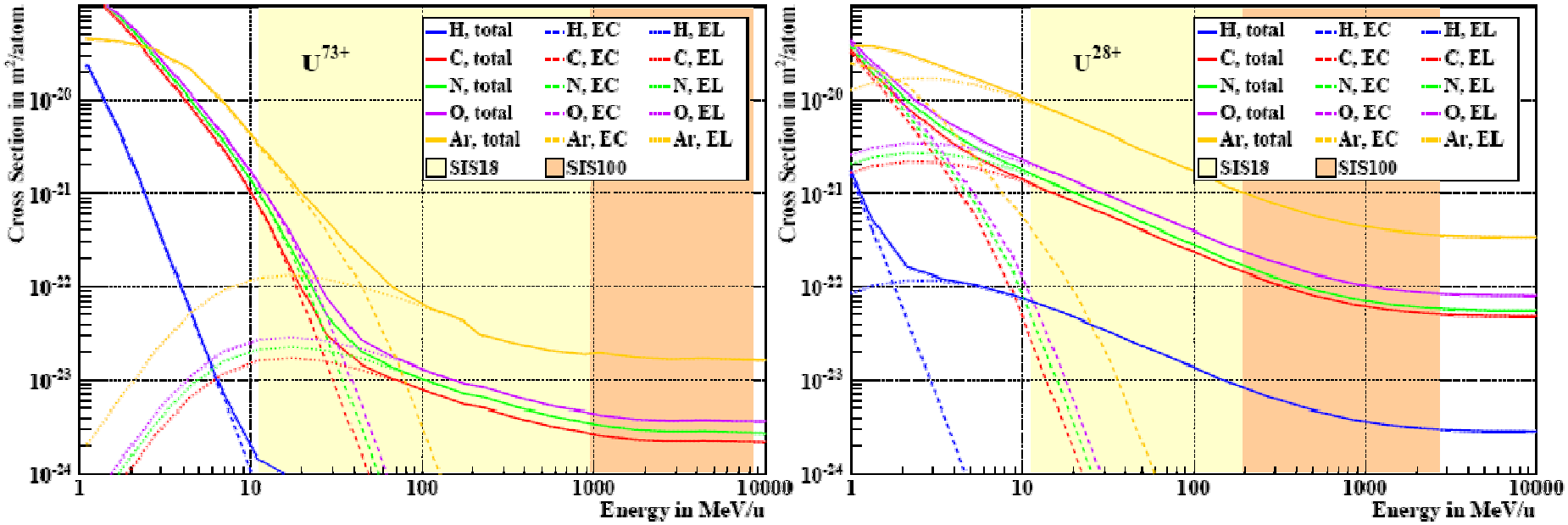

Heavy residual gas components must be avoided!

Example for Dynamic Vacuum

Simulation for SIS18, $2 \cdot 10^{10}$ U^{28+} injected, different amount of losses at injection

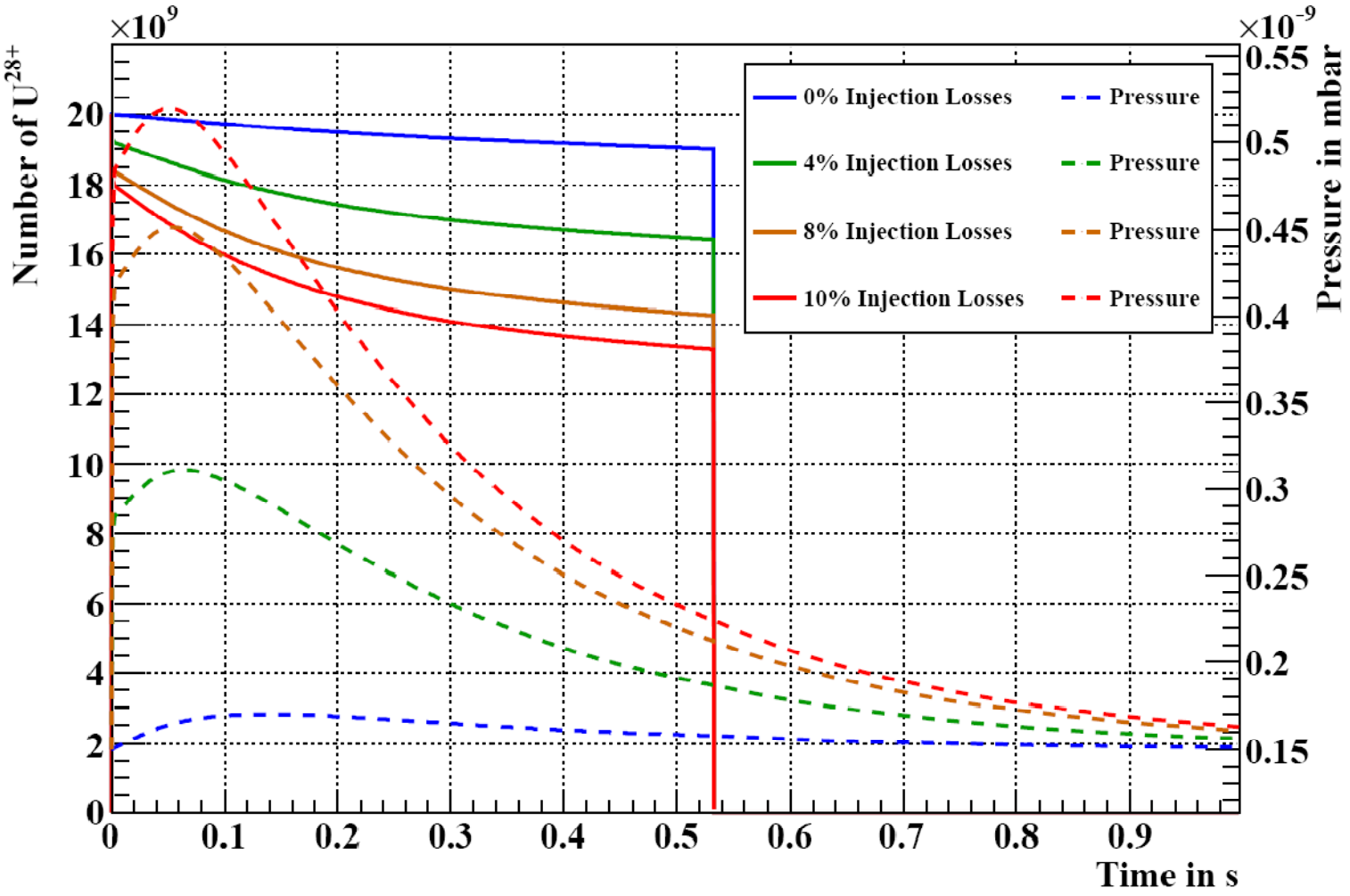

SIS100 Loss Distribution

Normalized losses in one arc, $U^{28+} \rightarrow U^{29+}$

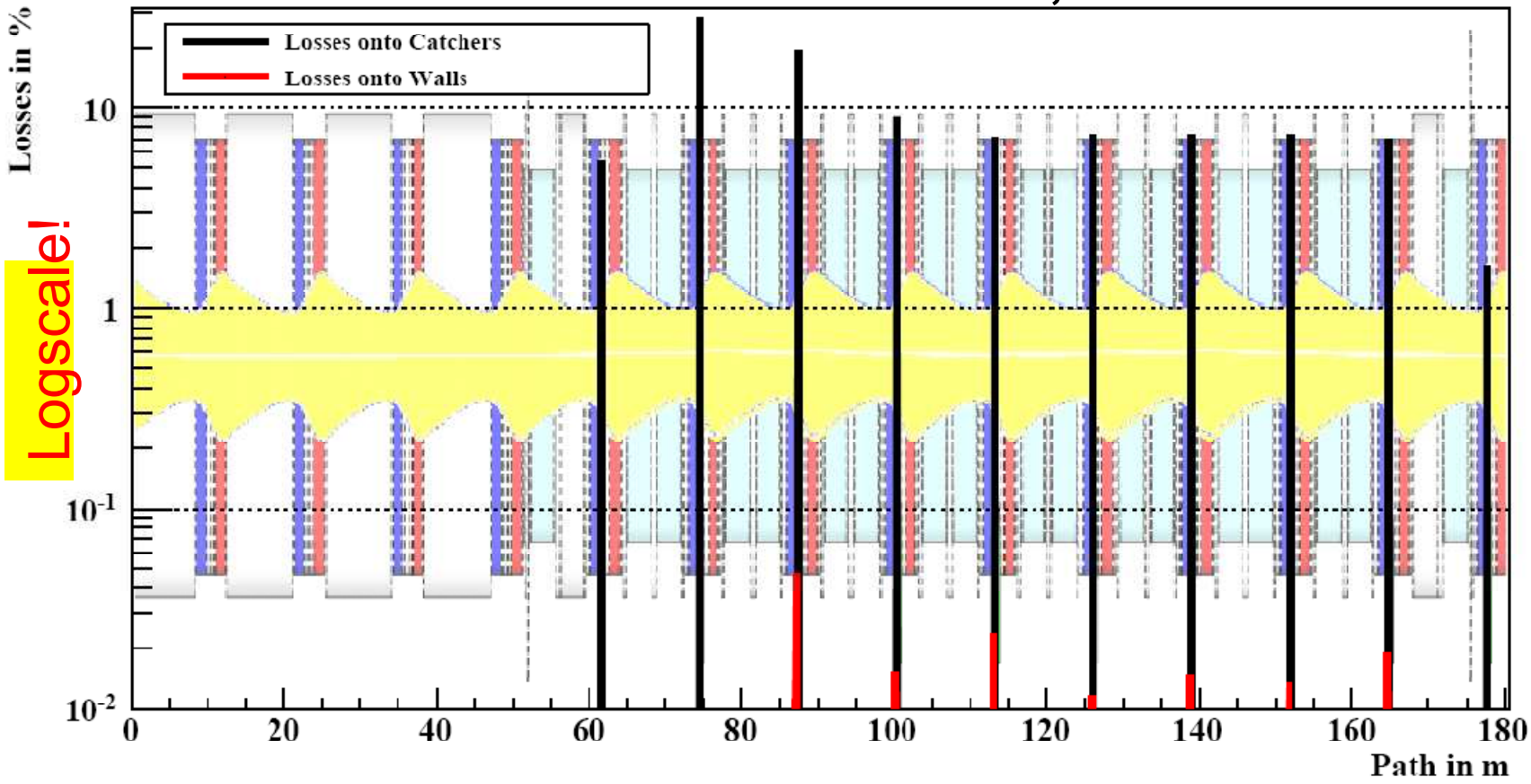

SIS100 Catching Efficiency

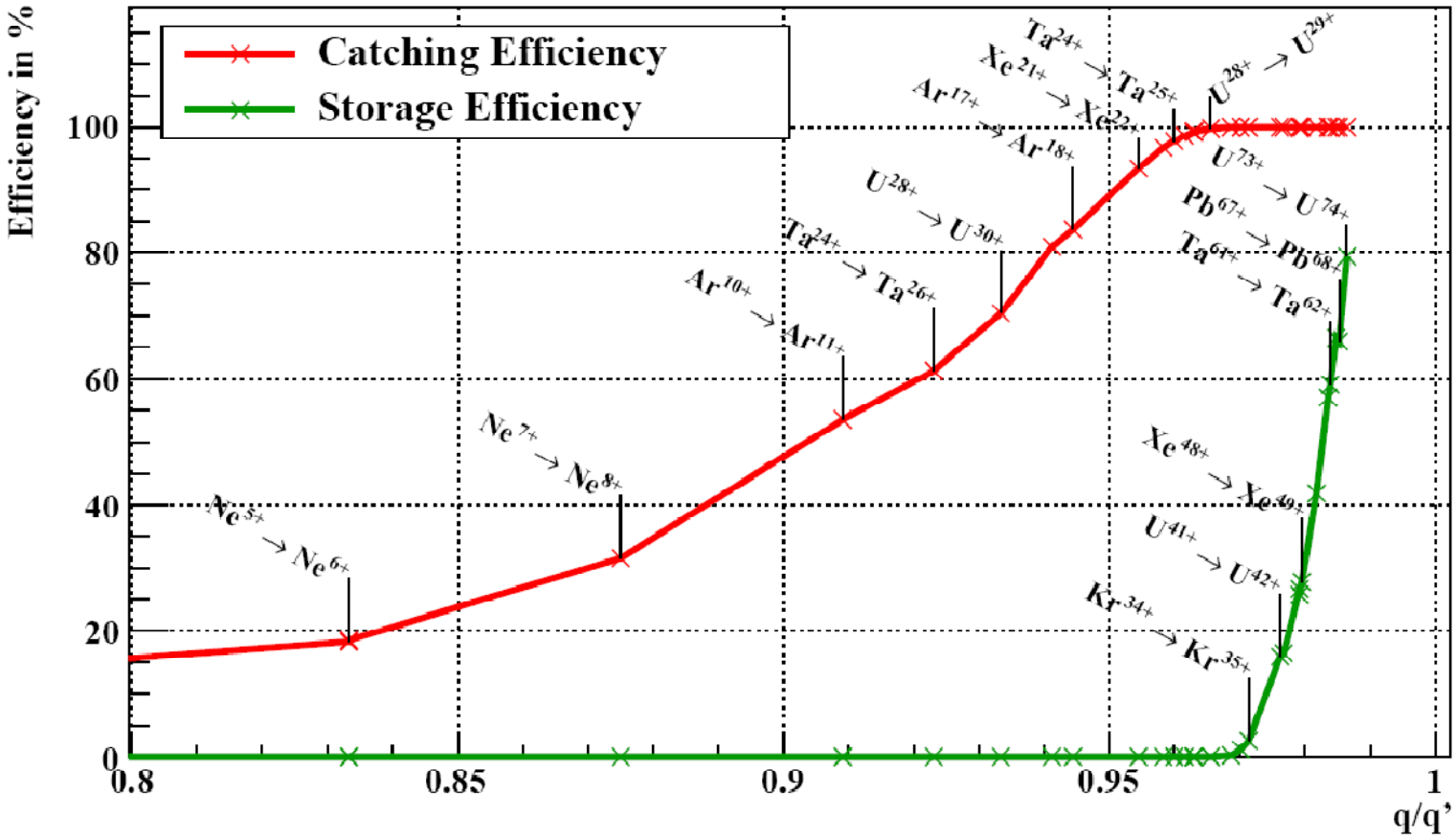

SIS100 Simulation

- Injection of 4 x $1.5 \cdot 10^{11}$ U^{28+} particles
- Base pressure $5 \cdot 10^{-12}$ mbar, residual gas Hydrogen dominated
- 10 K on all cold surfaces, effective pumping speed 74 m^3/s
- Desorption yield: 25500 (dE/dx scaled)
  (54.7% CO, 22% H_2, 16.4% CO_2, 4.1% CH_4, 2.8% N_2)
- Low energetic desorption yield: 5 (Target Ionization)
- Systematic losses at injection (2%), and extraction losses (2%)

SIS100 Simulation

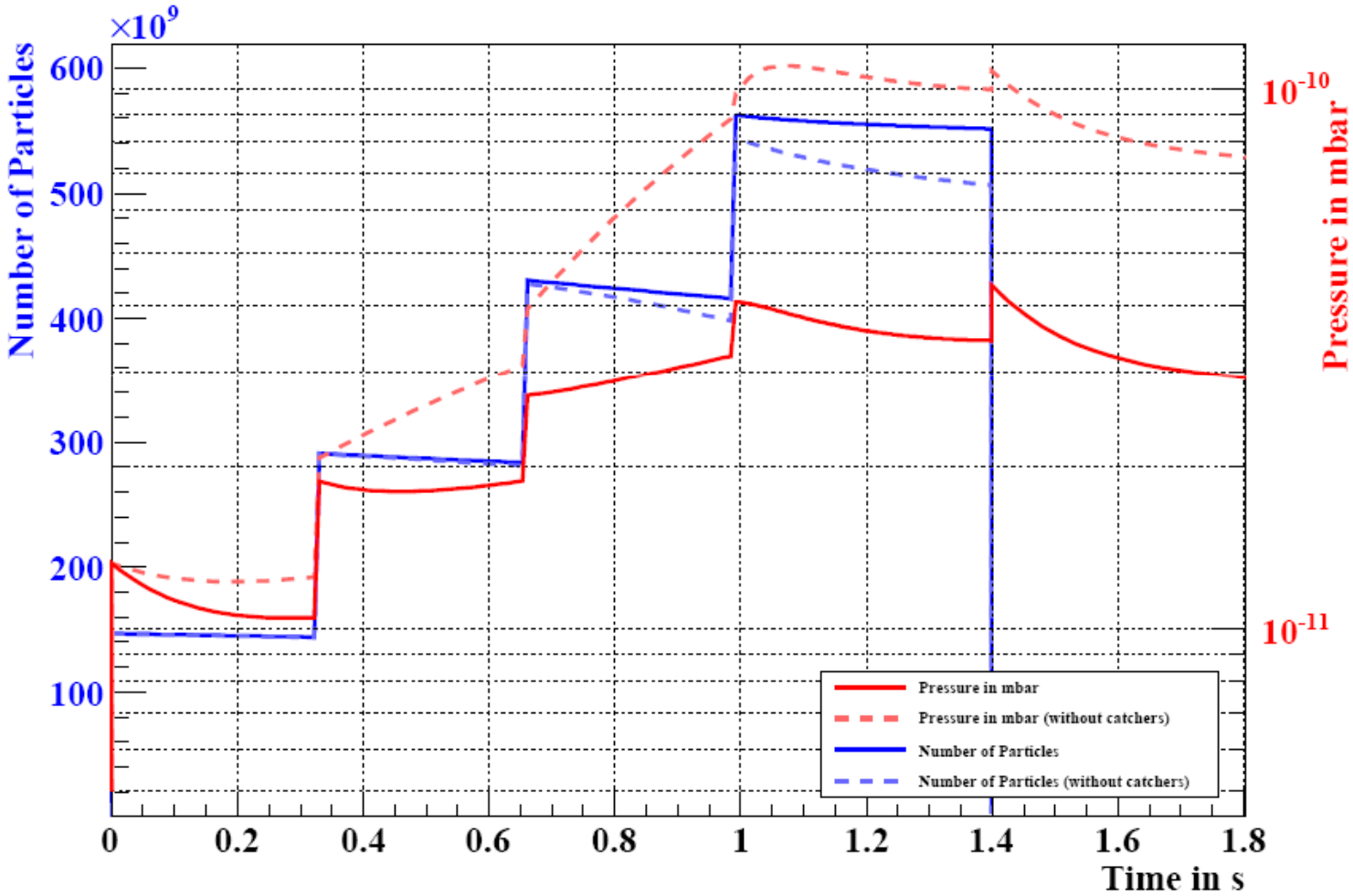

SIS18 Machine Experiment

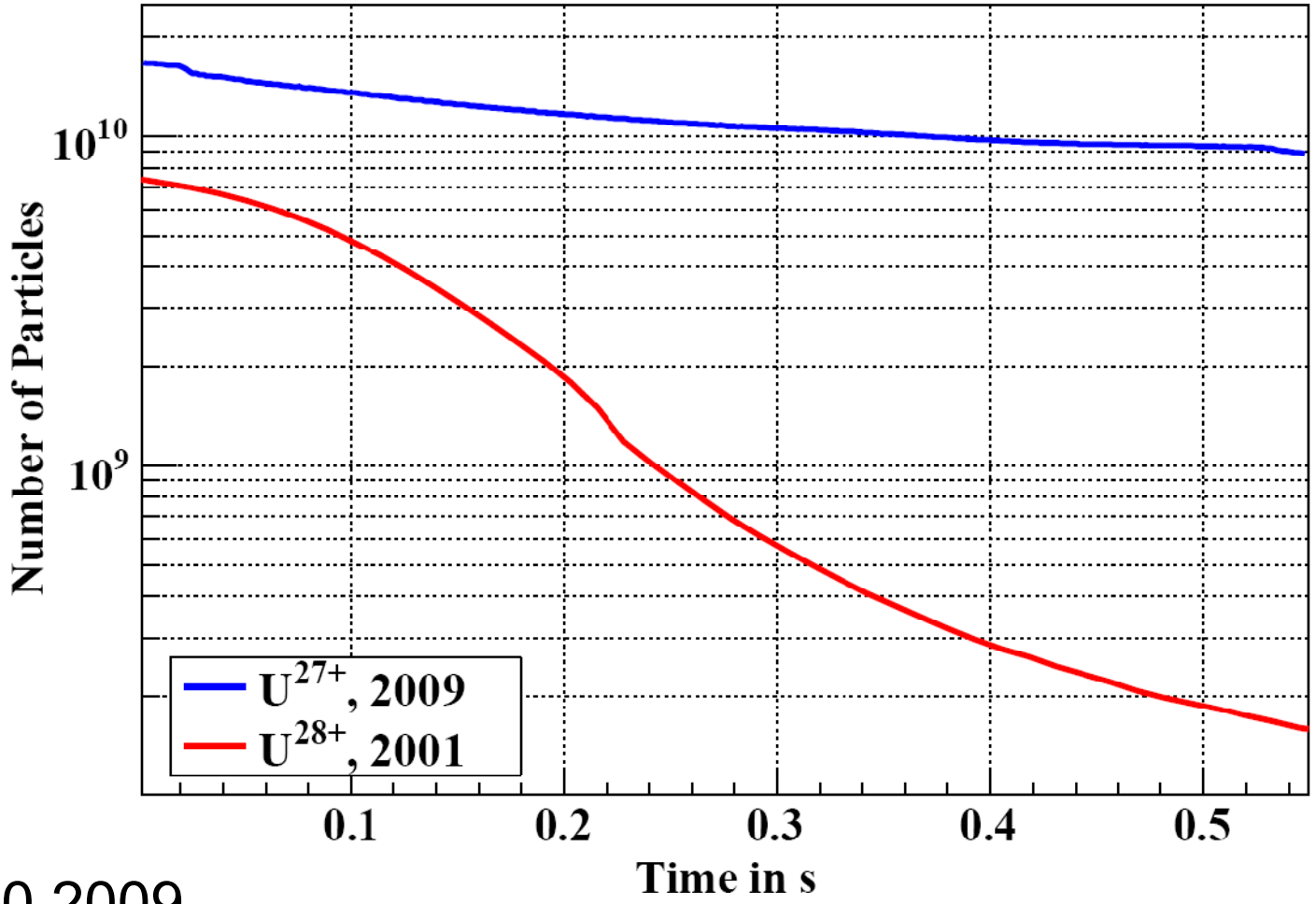

15.10.2009

Ion Catcher

- Controlled catching of ionized ions on low desorption surfaces
- Ions hitting the wall release adsorbed gases and produce a local pressure bump
  - Desorption yield is lowest for perpendicular incidence
  - Most ionized ions are caught by the ion catcher
  - Significant reduction of gas desorption

  → Dynamic residual gas pressure is stabilized

  → Lower total ionization loss

  - Activation and radiation damage of magnets by ionization beam loss is reduced

- SIS100 Ion Catcher is part of the EuCARD WP8: ColMat

Cryo-Catcher for Ionization Beam Loss

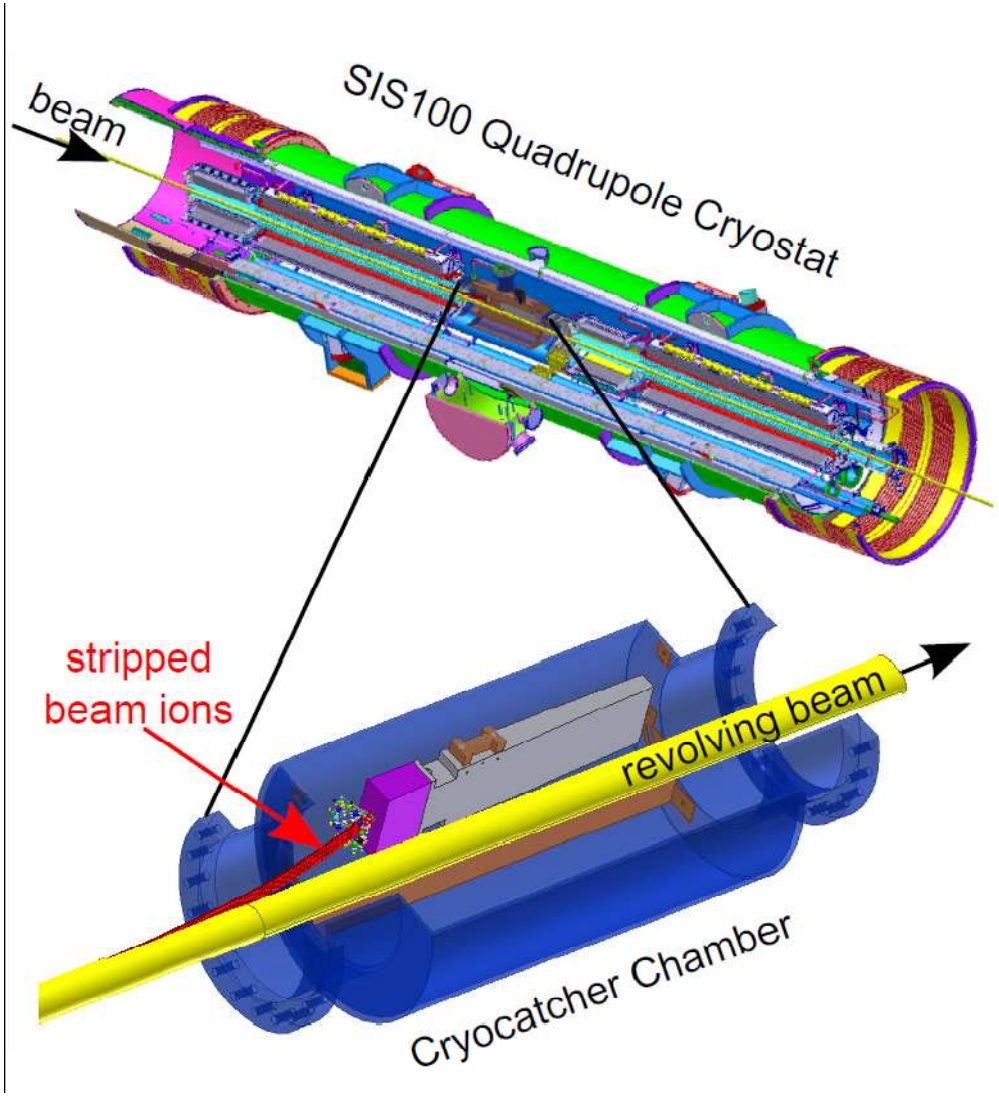

66 cryo-collimators foreseen in the SIS100 arcs for the suppression and control of desorption gases

Collaboration between GSI and CERN in the frame of EU FP7 COLMAT

GSI: Work package leader

- Different geometries
- Different temperatur levels
- Test with beam at GSI facility
- Effective desorption yield
- Pumping properties for the different residual gas components

WDM Experiments

An intense heavy ion beam is an excellent tool to generate HED/WDM samples

- Fairly uniform physical conditions
- Large heated volume (mm^3)
- High repetition rate and reproducibility
- Any target material

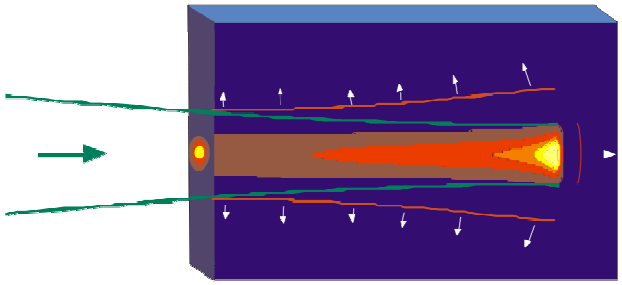

Scheme of ion-beam heated target

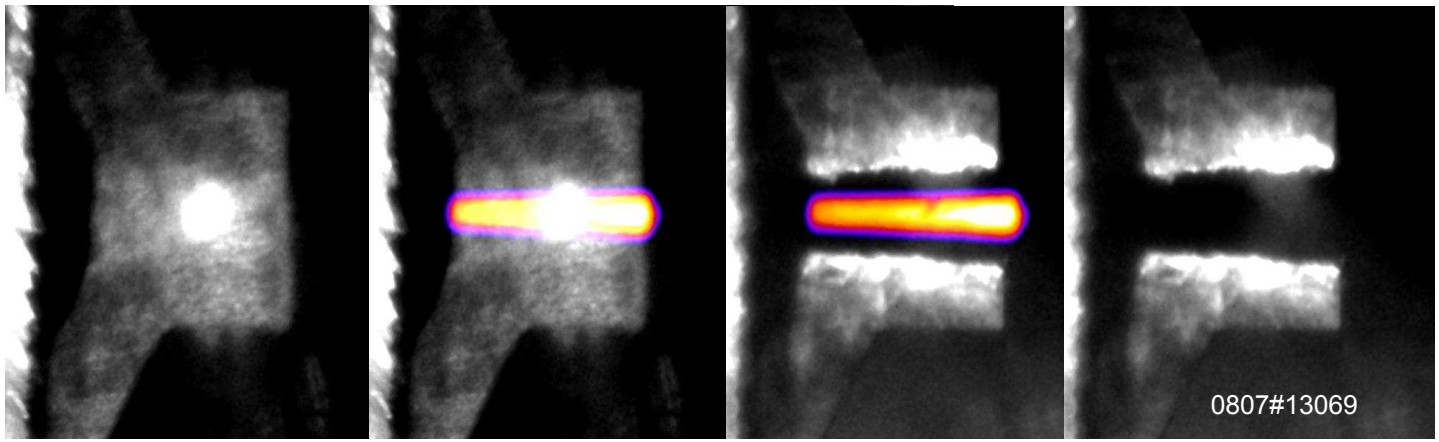

D.Varentsov,
A. Hug

HHT experimental area at GSI

- $^{238}U^{73+}$ or $^{128}Xe^{54+}$, 350 AMeV, e^- - cooled, up to $4 \cdot 10^9$ ions in 0.1 … 0.9 µs
- <300 µm spot on target, specific energy up to 5 kJ/g
- Temperature up to 2 eV, pressure in multi-kbar range
- Various target materials:
  W, Ta, Pb, Cu, Al, Au, Sn, C, ...
  Al_2O_3, UO_2, LiF, SiO_2, ...

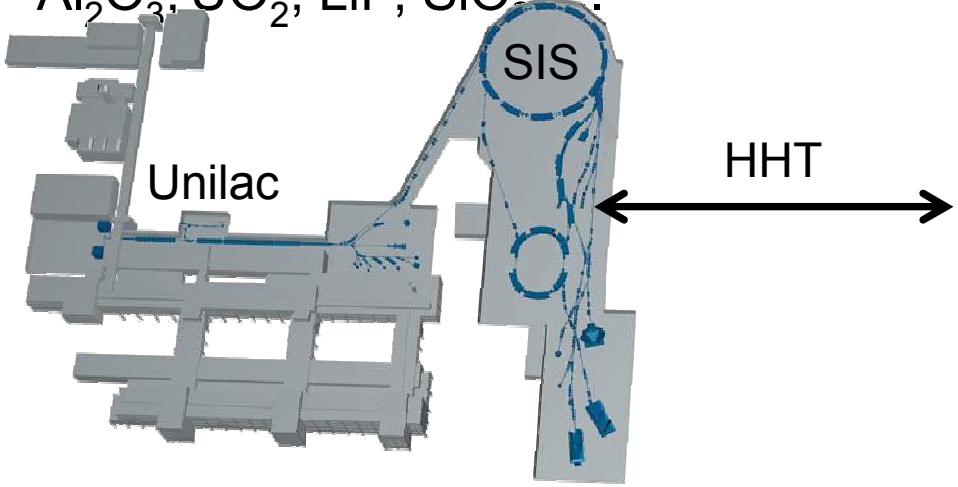

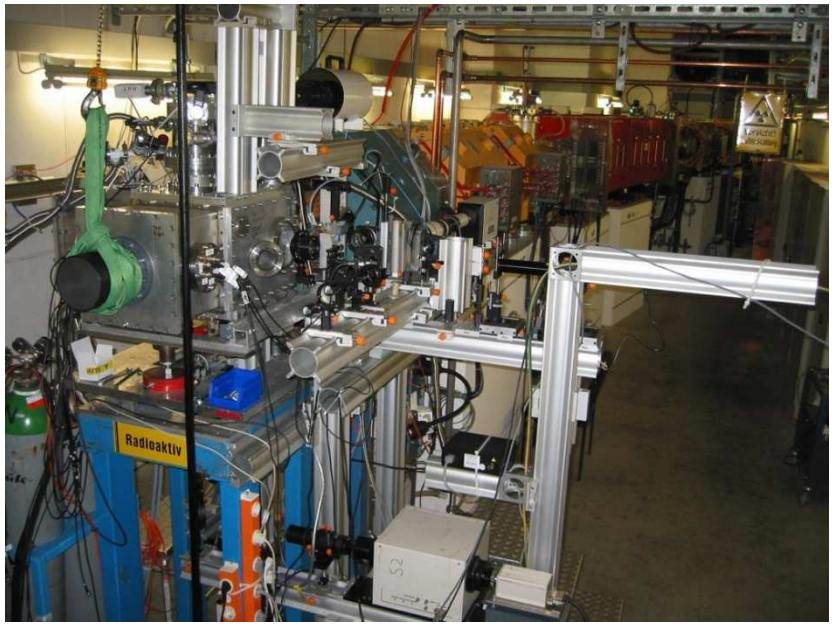

Recent experiments at HHT

- Reflectivity/ emissivity and electrical conductivity of refractory metals at melting and in hot,expanded liquid states
- Laser-diode reflectometer embedded into multi-channel pyrometer setup
- Fully integrated 4-point conductivity measurements
- Tests of noncontact techniques
- Opacity of thin WDM layers (C, Au, Al)
- Beam diagnostic at interaction point
- Spectroscopic studies of gas-targets
- Concentrate on two target materials: tungsten, tantalum
- From single-shot experiments towards reproducibility and statistics

Reflectivity measurements of ion beam heated refractory metals

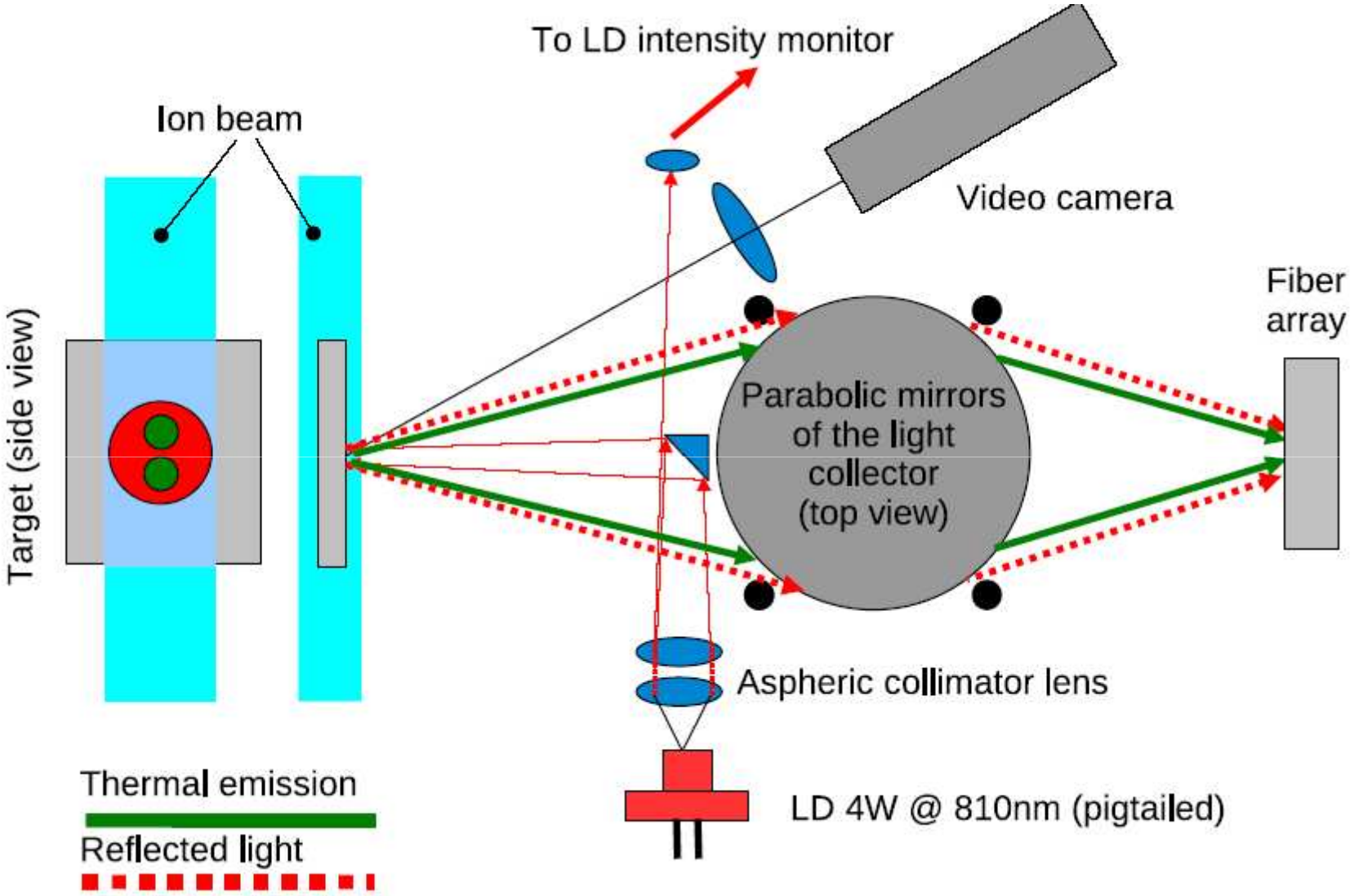

Reflectometer embedded in multi channel pyrometer

Fast multi-channel pyrometer

- Two spectral analyzers with 6 channels each (Vis/NIR)
- Spatial resolution down to 50µm, defined by fiber
- Absolute calibrated
- Embedded reflectometer with diffusive light collector

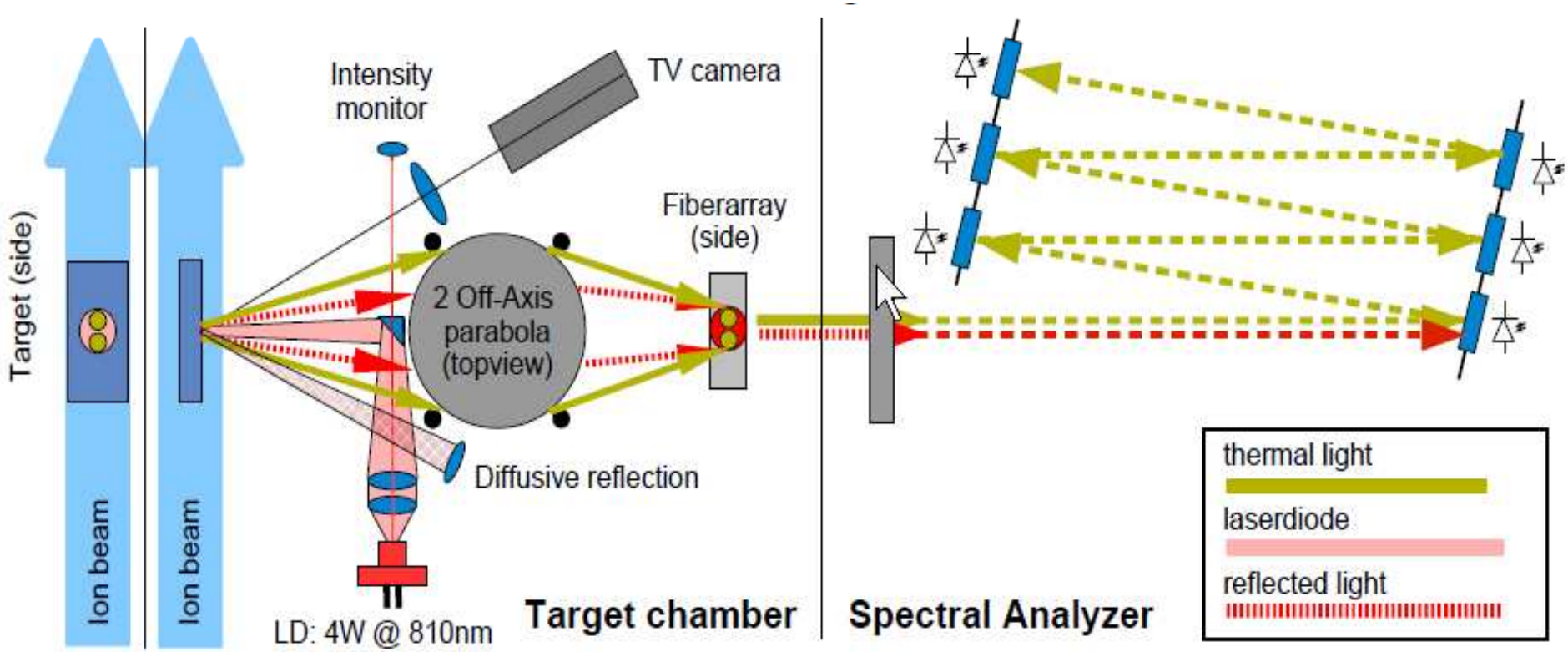

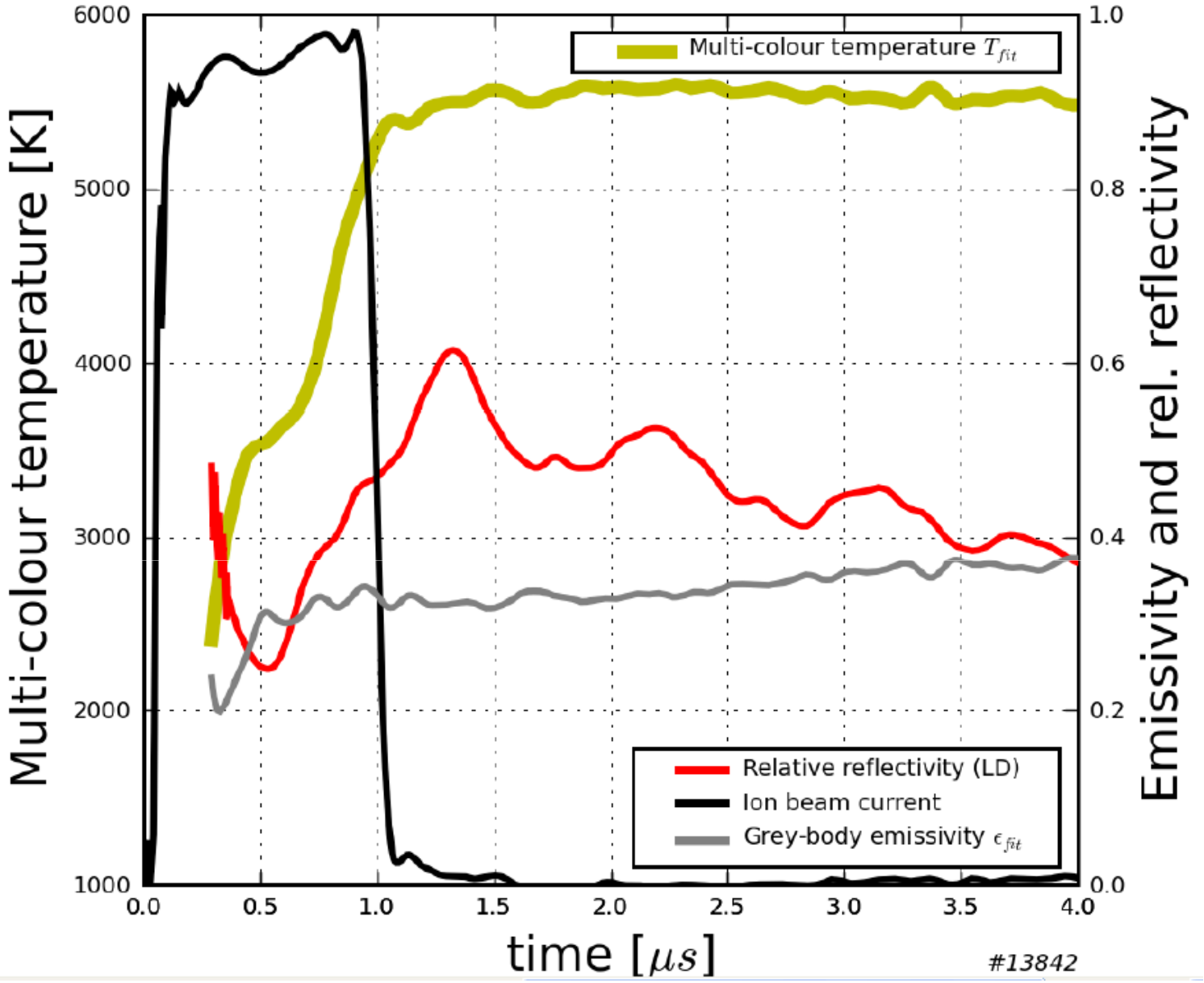

Multi color temperature and grey body emissivity along with relative reflectivity on a Tungsten target

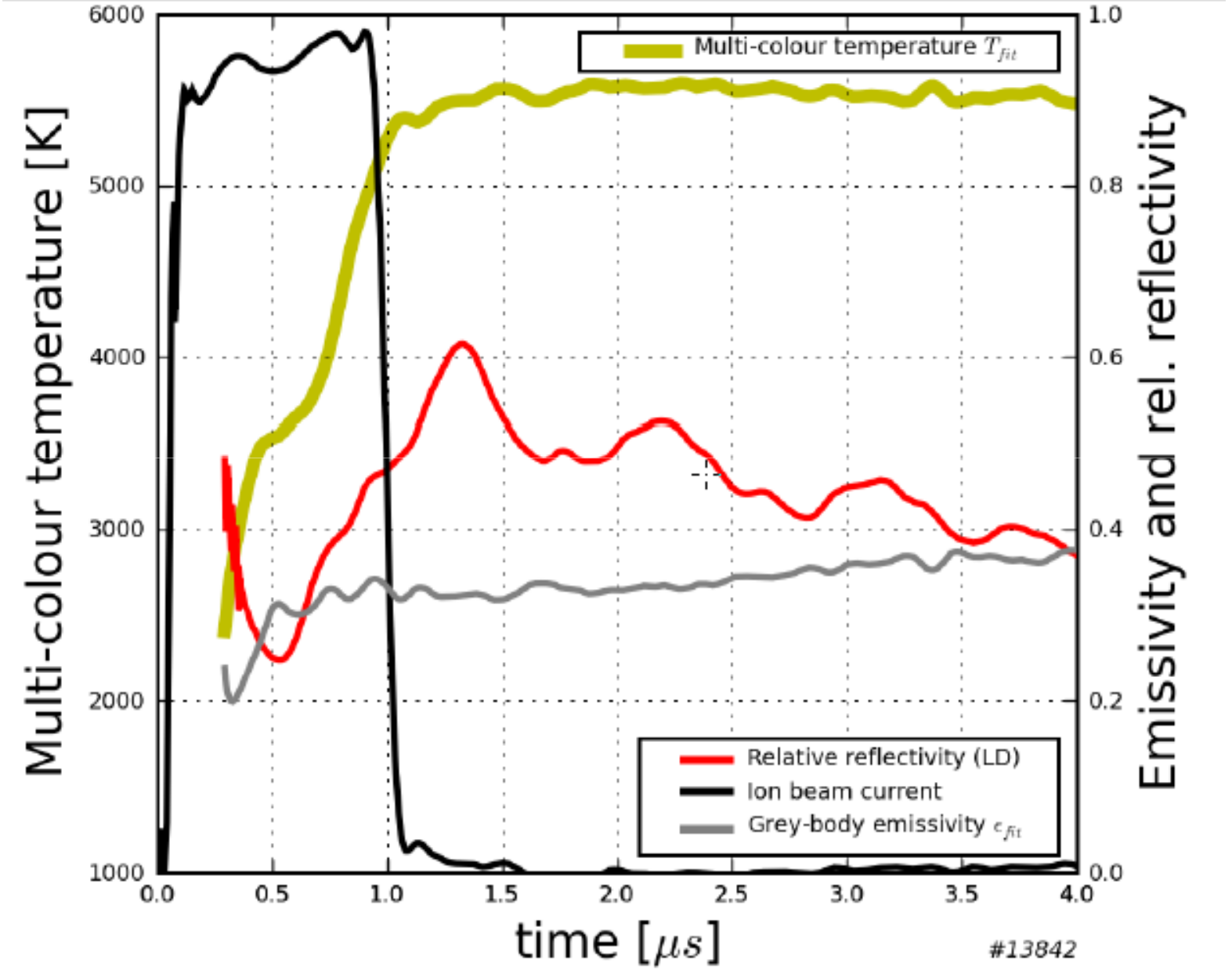
Multi-colour temperature T_{fit}
Relative reflectivity (LD)
Ion beam current
Grey-body emissivity ϵ_{fit}
Multi-colour temperature [K]
Emissivity and rel. reflectivity
time [μs]
#13842
6000
5000
4000
3000
2000
1000
1.0
0.8
0.6
0.4
0.2
0.0
0.0
0.5
1.0
1.5
2.0
2.5
3.0
3.5
4.0

Enthalpy calculation

- Transforming time axis to enthalpy axis
  - Ion beam current from fast current transformer
  - Temperature and enthalpy values at end of melting from literature

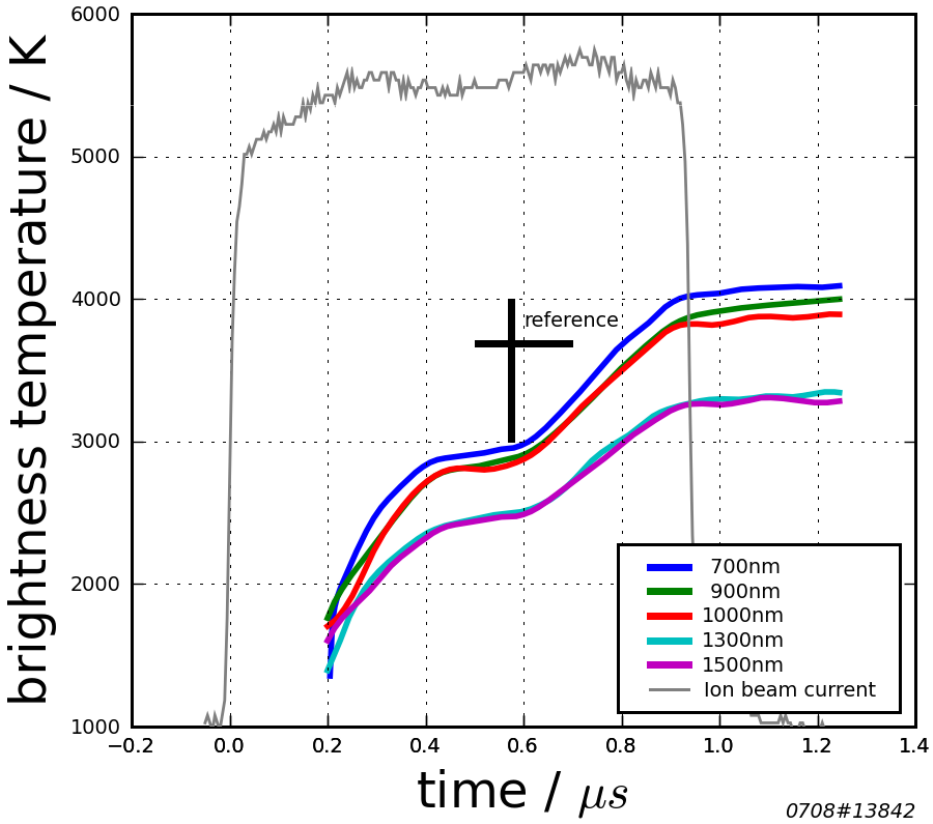

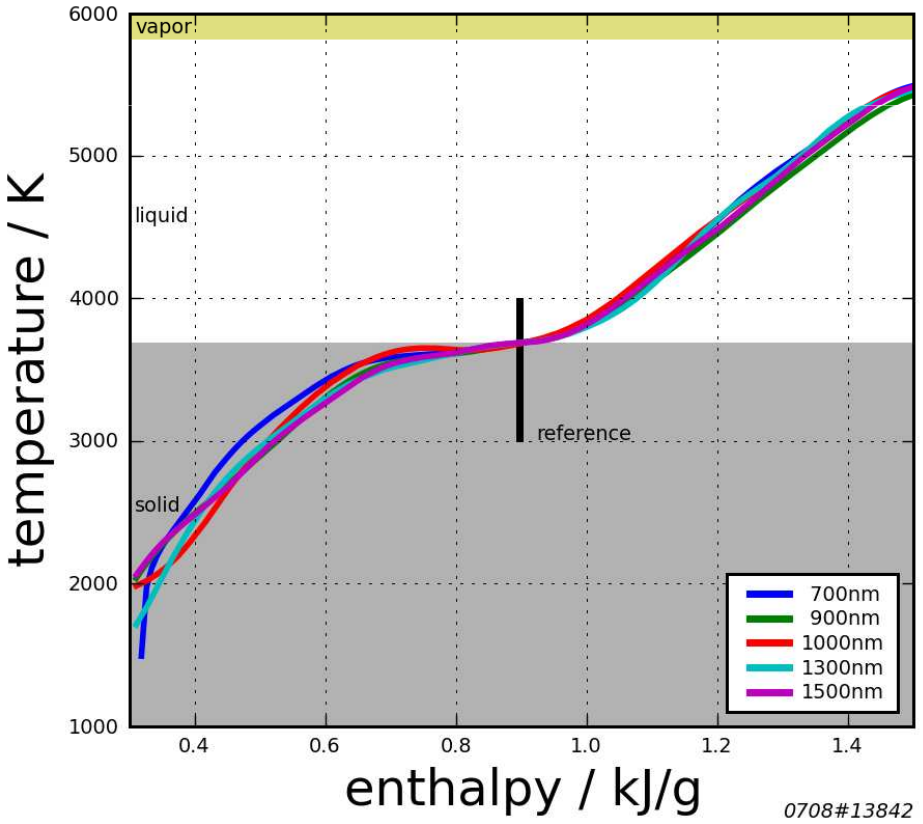

Statistics

- One experimental campagne
- Accumulating 17 shots on tantalum, 20 shots on tungsten

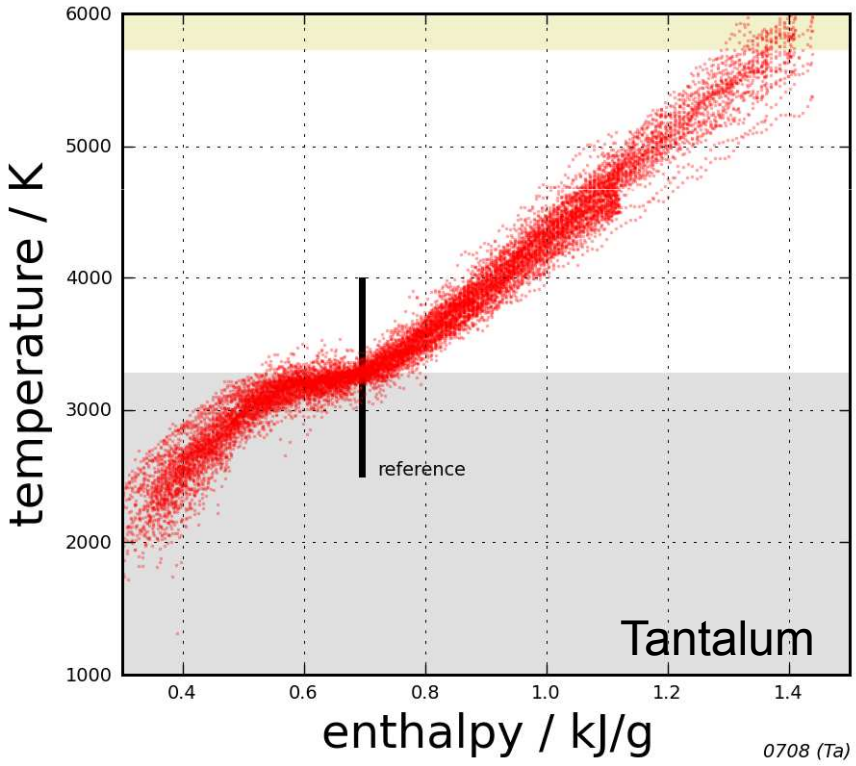

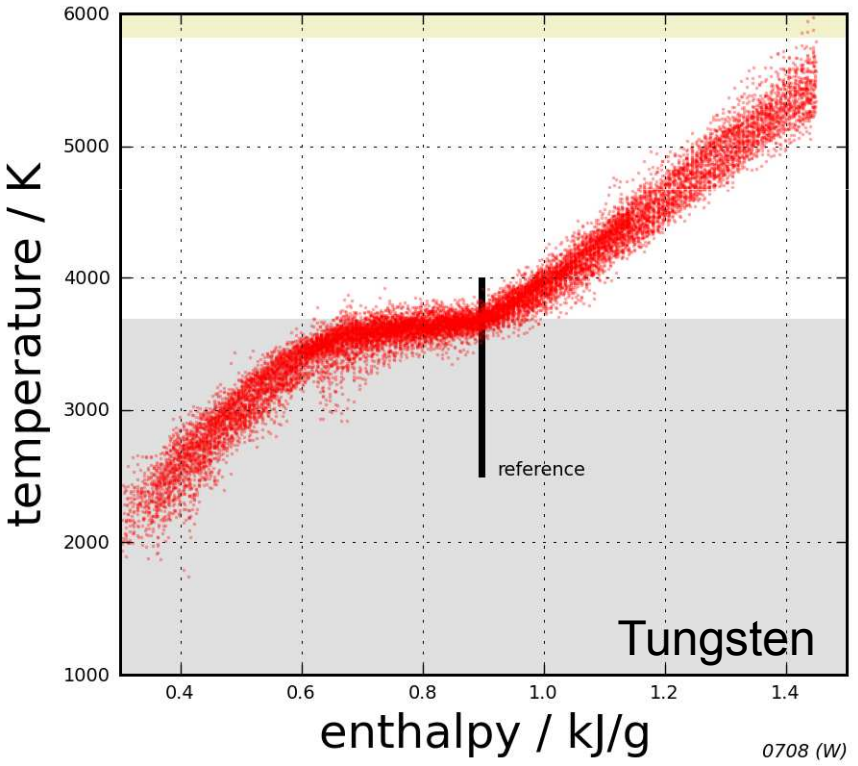

Heat capacity

- Linear fitting results in heat capacity, assuming no temperature dependency in solid state and after melting

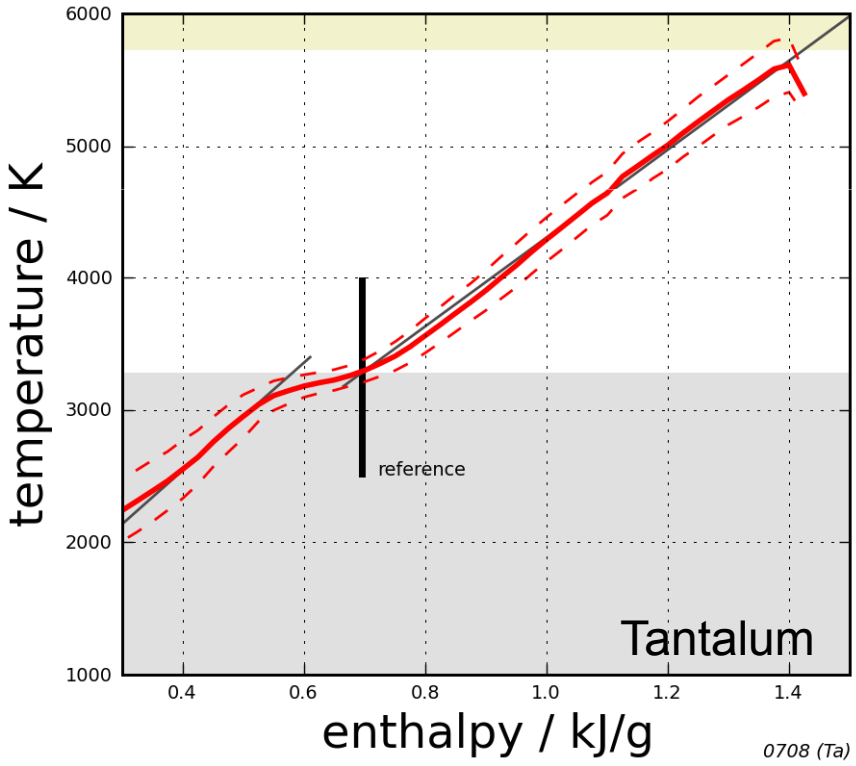

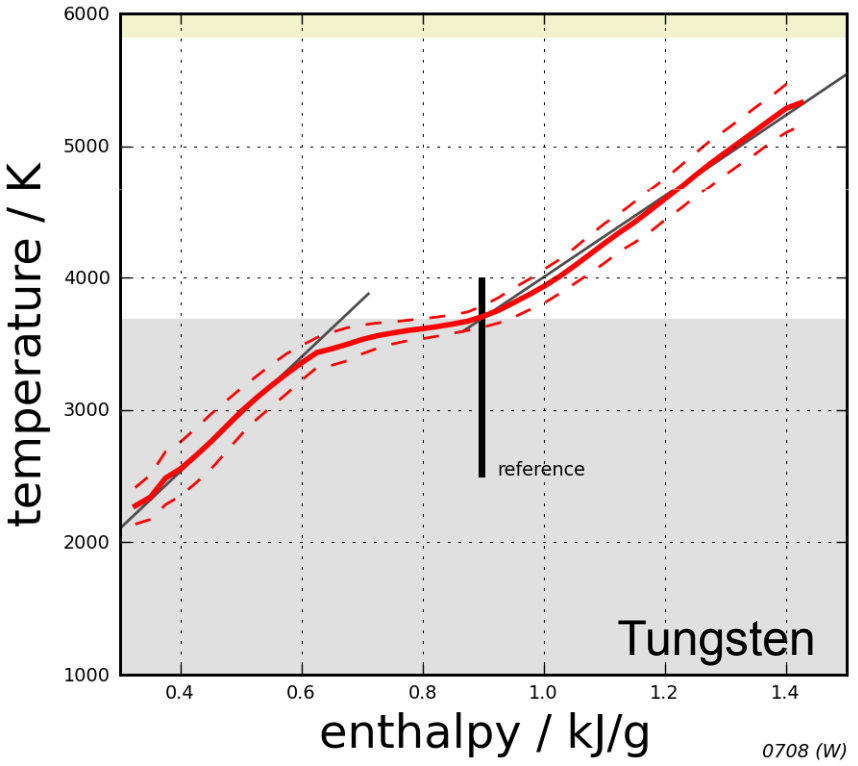

Results

- Calculating the mean value and standard deviation

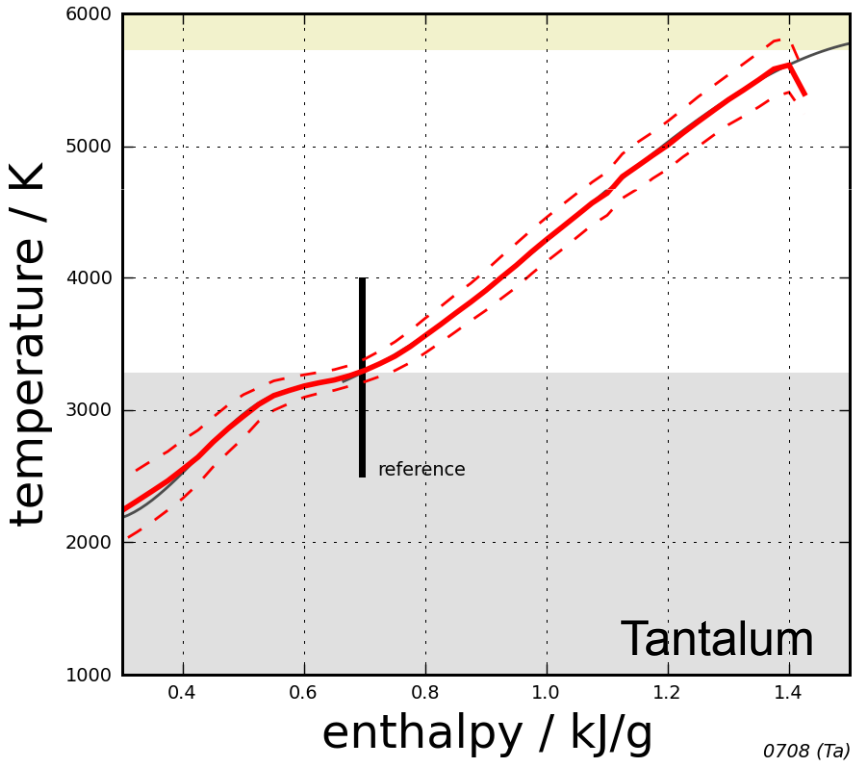

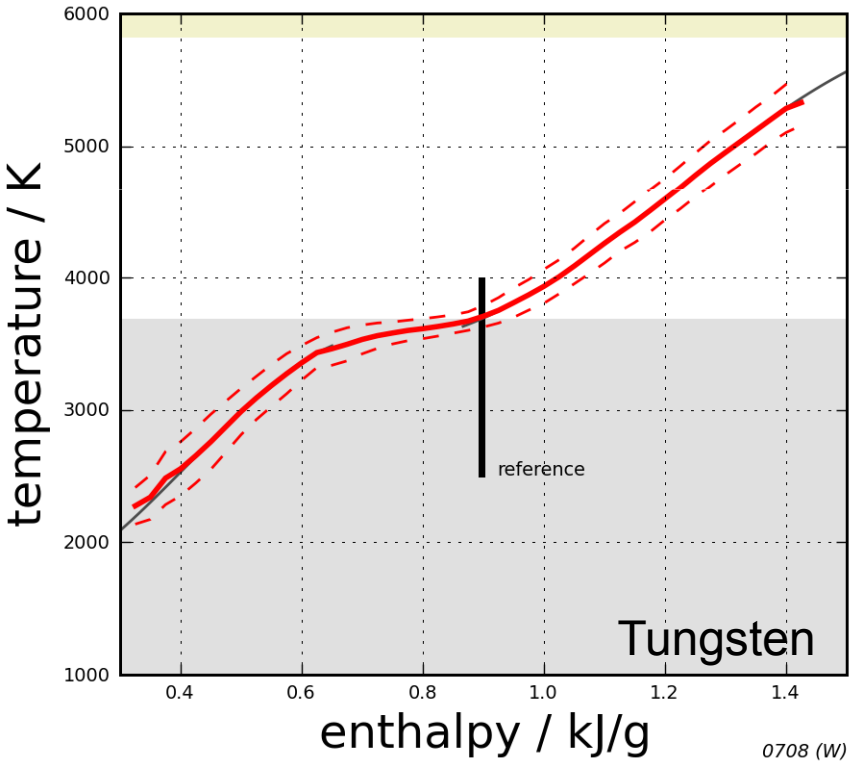

Discussion and outlook

- Transforming time to enthalpy using literature values for temperature and enthalpy at end of melting
  - Independent of beam intensity, target geometry, surface conditions
  - Source of error: finding the point of start and end of melting
- Several shots on tantalum and tungsten allow statistics and to calculate:
  - Melting enthalpy
  - Heat capacity in solid and liquid state
- Comparison to reported values in god agreement
- Next steps
- Process volume increase (streak)
- Calculate emissivity change (multi-channel pyrometer)
  - Decrease spread
  - Compare specular and diffusive reflected light with emissivity

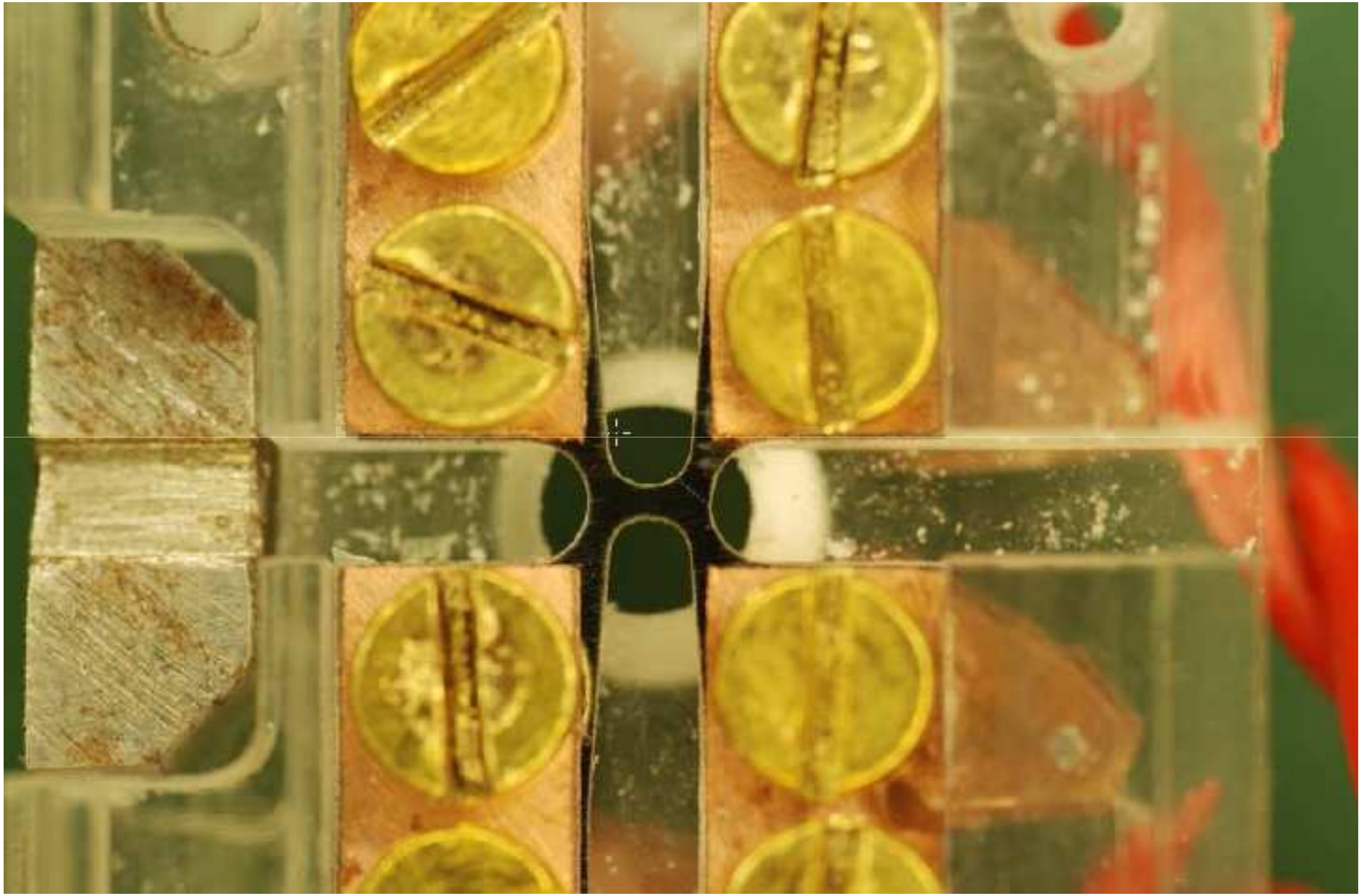

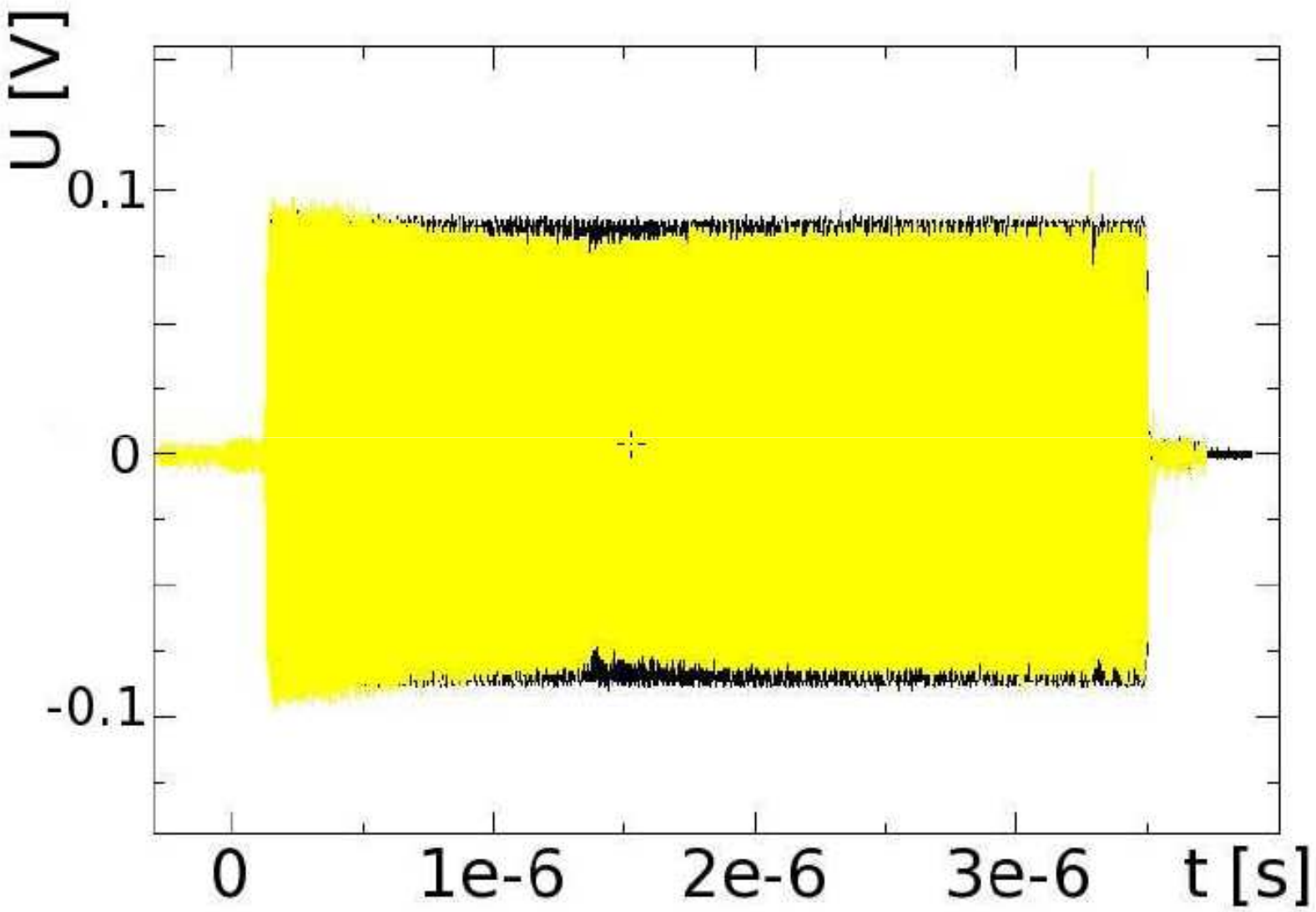
U [V]
0.1
0
-0.1
0
1e-6
2e-6
3e-6
t [s]

Contactless Electrical Conductivity Measurements by Eddy Currents